Anal. Chem. **2005,** *77,* 6864−6873

Microarray Immunoassay for Phenoxybenzoic Acid Using Polymer Encapsulated Eu:Gd_2O_3 Nanoparticles as Fluorescent Labels

Mikaela Nichkova,[†] Dosi Dosev,[‡] Shirley J. Gee,[†] Bruce D. Hammock,[†] and Ian M. Kennedy*[,‡]

Department of Entomology and Department of Mechanical and Aeronautical Engineering, University of California Davis, One Shields Avenue, Davis, California 95616

Currently, detection in microarray bioanalysis is based mainly on the use of organic dyes. To overcome photobleaching and spectral overlaps we applied a new type of fluorophore, crystalline europium-doped gadolinium oxide (Eu:Gd_2O_3) nanoparticles, as labels in immunoassay microarrays. The Eu:Gd_2O_3 nanoparticles synthesized by spray pyrolysis offer narrow red emission, large Stokes shift, photostable laser-induced fluorescence with a long lifetime (1 ms). The amino functionalization of the particles was achieved by poly(L-lysine) (PL) encapsulation. The formation of a stable PL shell was confirmed by TEM analysis, colloidal stability studies, and quantification of the surface reactive amino groups. The PL-encapsulated particles were covalently conjugated to antibodies and successfully applied as reporters in a competitive fluorescence microimmunoassay for phenoxybenzoic acid (PBA), a generic biomarker of human exposure to pyrethroid insecticides. Microarrays were fabricated by microcontact printing of BSA−PBA in line patterns (10 × 10 μm). Confocal fluorescence microscopy combined with internal standard (fluorescein) calibration was used for quantitative measurements. The microarray immunoassay demonstrated a limit of detection of 1.4 $\mu g\ L^{-1}$ PBA. This work suggests the potential application of lanthanide oxide nanoparticles as fluorescent probes in microarray and biosensor technology, immunodiagnostics, and high-throughput screening.

Protein microarrays have the potential to play a fundamental role in the miniaturization of biosensors, high-throughput drug screening, clinical immunological assays, and protein−protein interaction studies. Improved labeling and detection technologies are a prerequisite for optimal miniaturization. Microarrays are usually visualized and analyzed using organic fluorescent dyes.[1] Organic fluorophores, however, have some characteristics, such as spectral overlaps and poor photostability, that limit their effectiveness in such applications. Dye photobleaching can also reduce significantly the available time for imaging, and this is why photostability of the fluorescent labels is of crucial importance for this type of application. Therefore, it is highly desirable to develop new fluorescent probes for microarray-based bioanalysis.

Efforts to improve the performance of immunosensing by incorporating different kinds of novel nanostructures (polymer beads, fluorophore-doped nanoparticles, semiconductor quantum dots, inorganic and organic nanoparticles) have gained a lot of attention in recent years (for a review see Seydack[2]). Fluorescent lanthanide chelates have been shown to provide 100−1000-fold better sensitivities in comparison with conventional fluorophores because of efficient background fluorescence rejection achieved through their large Stokes shifts, narrow emission bands, time-resolved fluorometric measurements and lack of quenching when multiple labeling is used.[3,4] One of the main drawbacks of lanthanide chelates—the fluorescence quenching by water molecules—has been overcome by incorporating the chelates into polymer beads where the polymer shell efficiently removes the water from the vicinity of the chelates by producing a hydrophobic environment. Thus, europium chelates encapsulated by polystyrene nanoparticles have been shown to be suitable labels for ultrasensitive immunoassays where detection limits of zeptomoles for prostate-specific antigen (PSA) have been obtained.[5,6] Recently, time-resolved fluorescence microscopy using Eu chelate-containing polystyrene nanoparticles has been applied for quantitative histochemistry measurements of PSA in biological samples.[7] However, some factors such as photobleaching, the high cost of preparation, a tendency to agglomerate in an aqueous medium due to their hydrophobic property, swelling, and dye leaking still prevent their use in routine bioanalysis. Lanthanide chelate-doped silica nanoparticles offer the advantages of smaller size, high hydrophilicity, biocompatibility, and photostability and can be relatively easily modified to attach biomolecules. Very sensitive sandwich immunoassays have been recently developed using these particles as reporters.[8−10]

* Corresponding author. E-mail: imkennedy@ucdavis.edu. Phone: 1530 752-2796. Fax: 1 530 210-8220.

[†] Department of Entomology.

[‡] Department of Mechanical and Aeronautical Engineering.

(1) Bernard, A.; Renault, J. P.; Michel, B.; Bosshard, H. R.; Delamarche, E. *Adv. Mater.* **2000**, *12*, 1067−1070.

(2) Seydack, M. *Biosens. Bioelectron.* **2005**, *20*, 2454−2469.

(3) Diamandis, E. P.; Christopoulos, T. K. *Anal. Chem.* **1990**, *62*, 1149A−1157A.

(4) Scorilas, A.; Bjartell, A.; Lilja, H.; Moller, C.; Diamandis, E. P. *Clin. Chem.* **2000**, *46*, 1450−1455.

(5) Harma, H.; Soukka, T.; Lovgren, T. *Clin. Chem.* **2001**, *47*, 561−568.

(6) Huhtinen, P.; Soukka, T.; Lovgren, T.; Harma, H. *J. Immunol. Methods* **2004**, *294*, 111−122.

(7) Vaisanen, V.; Harma, H.; Lilja, H.; Bjartell, A. *Luminescence* **2000**, *15*, 389−397.

(8) Tan, M. Q.; Wang, G. L.; Hai, X. D.; Ye, Z. Q.; Yuan, J. L. *J. Mater. Chem.* **2004**, *14*, 2896−2901.

10.1021/ac050826p CCC: $30.25
Published on Web 09/23/2005

Inorganic semiconductor nanocrystals (quantum dots) are also very attractive for biolabeling due to their properties such as excellent brightness, narrow and precise tunable emission, negligible photobleaching, fairly high quantum yields, and photostability.[11,12] Although quantum dots have proven to be suitable labels for biological imaging[13,14] and DNA microarray analysis,[15] their application in quantitative immunoassays is still limited. Some of the limitations are mainly due to poor solubility in water (unless they are modified), agglutination, photoblinking, high-cost production, and concerns regarding toxic cadmium and lead components. Furthermore, their luminescent properties are strongly dependent on their size, surface modification, and the chemical environment.

Lanthanide oxides are commonly used as fluorescent materials in the lighting industry.[16,17] Surprisingly, these nanoparticles have received little attention for biological applications.[18,19] Crystalline europium oxide (Eu_2O_3) nanoparticles have been used as a fluorescent label in a competitive immunoassay with magnetic separation for the herbicide atrazine with a detection limit comparable to that of the respective ELISA.[18] Here we propose the use of lanthanide ion-doped oxide nanoparticles as a promising new class of biological fluorescent labels in microarray immunoassays. Like chelates, the nanoparticles of lanthanide oxides offer large Stokes shifts, narrow emission bandwidths, and long fluorescence lifetime (about 1−2 ms). In addition, they possess inherent photostability. In contrast to semiconductor quantum dots, the emission wavelength of the lanthanide oxide nanoparticles is independent of the particle size and hence monodispersity is less crucial, leading to lower costs of synthesis. Their optical properties are not much influenced by the surface coating because their fluorescence is due to electronic transitions of the dopant. No blinking behavior is expected owing to the large number of dopant ions in one nanoparticle. Furthermore, the synthesis of lanthanide oxides can be quick, simple, and scalable for mass production. Particles with different emission wavelengths can be easily obtained by controlled doping of lanthanide ions into an appropriate host material making them suitable for multicolor labeling.[20]

The potential application of nanomaterials as biolabels has led to a lot of effort directed toward their efficient biofunctionalization. Silanization by a variety of functionalized alkoxysilanes has been the most commonly used procedure for surface modification of luminiphore-doped silica,[9,21] Eu_2O_3 nanoparticles,[18] and CdTe and gold nanocrystals.[22] Silanization suffers from aggregation of particles, nonspecific adsorption of proteins in bioassays and it is a time-consuming process that sometimes is difficult to reproduce.[18] An alternative coating method is based on the spontaneous physical adsorption of proteins on the nanoparticle surface due to hydrophobic or electrostatic forces. It has been applied to dye-doped silica nanoparticles,[23] fluorescein diacetate nanoparticles,[24] silole nanocrystals,[25] and quantum dots.[26−29] In our previous works, we have used a similar direct coating method for the biofunctionalization of Eu^{3+}-doped gadolinium oxide (Eu:Gd_2O_3) nanoparticles with a variety of proteins (avidin, BSA−biotin, IgG), and we have demonstrated their application as fluorescent labels for micropattern imaging for the avidin−biotin[30] and anti-rabbit IgG/rabbit IgG[31] systems. Although the direct coating is a one-step procedure, providing stable conjugates with proteins retaining their biological activity, its major drawback is the random immobilization of the receptors on the nanoparticle surface. An alternative surface functionalization (e.g., with amino groups) would allow the oriented covalent immobilization of antibodies through the carbohydrate moiety of the Fc region, resulting in a more reproducible number of binding sites on the surface of the nanoparticles. Electrostatic interactions between nanoparticles and oppositely charged polymers has been also extensively exploited.[32−35] It has been demonstrated that the polycationic poly(L-lysine) (PL; $pK_a \sim 10$) adsorbs tightly (primarily via the electrostatic interaction) to negatively charged surfaces, such as glass and silicon oxide substrates, glass beads,[36] silicon oxide particles, and a variety of metal oxide surfaces (Nb_2O_5, Ta_2O_5, TiO_2, SiO_2).[37] As a result of the similarity of the surface properties of these materials to the Gd_2O_3 surface, poly(L-lysine) was selected in this work as an adsorbing polycation for the amino functionalization of the Eu:Gd_2O_3 nanoparticles.

(9) Ye, Z. Q.; Tan, M. Q.; Wang, G. L.; Yuan, J. L. *Anal. Chem.* **2004**, *76*, 513−518.
(10) Ye, Z. Q.; Tan, M. Q.; Wang, G. L.; Yuan, J. L. *J. Mater. Chem.* **2004**, *14*, 851−856.
(11) Bruchez, M.; Moronne, M.; Gin, P.; Weiss, S.; Alivisatos, A. P. *Science* **1998**, *281*, 2013−2016.
(12) Chan, W. C. W.; Nie, S. M. *Science* **1998**, *281*, 2016−2018.
(13) Chan, W. C. W.; Maxwell, D. J.; Gao, X. H.; Bailey, R. E.; Han, M. Y.; Nie, S. M. *Curr. Opin. Biotechnol.* **2002**, *13*, 40−46.
(14) Jaiswal, J. K.; Simon, S. M. *Trends Cell Biol.* **2004**, *14*, 497−504.
(15) Gerion, D.; Chen, F. Q.; Kannan, B.; Fu, A. H.; Parak, W. J.; Chen, D. J.; Majumdar, A.; Alivisatos, A. P. *Anal. Chem.* **2003**, *75*, 4766−4772.
(16) Bhargava, R. N. *J. Lumin.* **1996**, *70*, 85−94.
(17) Tissue, B. M. *Chem. Mater.* **1998**, *10*, 2837−2845.
(18) Feng, J.; Shan, G. M.; Maquieira, A.; Koivunen, M. E.; Guo, B.; Hammock, B. D.; Kennedy, I. M. *Anal. Chem.* **2003**, *75*, 5282−5286.
(19) Beaurepaire, E.; Buissette, V.; Sauviat, M. P.; Giaume, D.; Lahlil, K.; Mercuri, A.; Casanova, D.; Huignard, A.; Martin, J. L.; Gacoin, T.; Boilot, J. P.; Alexandrou, A. *Nano Lett.* **2004**, *4*, 2079−2083.
(20) Gordon, W. O.; Carter, J. A.; Tissue, B. M. *J. Lumin.* **2004**, *108*, 339−342.
(21) Santra, S.; Zhang, P.; Wang, K. M.; Tapec, R.; Tan, W. H. *Anal. Chem.* **2001**, *73*, 4988−4993.
(22) Schroedter, A.; Weller, H.; Eritja, R.; Ford, W. E.; Wessels, J. M. *Nano Lett.* **2002**, *2*, 1363−1367.
(23) Tapec, R.; Zhao, X. J. J.; Tan, W. H. *J. Nanosci. Nanotechnol.* **2002**, *2*, 405−409.
(24) Chan, C. P. Y.; Bruemmel, Y.; Seydack, M.; Sin, K. K.; Wong, L. W.; Merisko-Liversidge, E.; Trau, D.; Renneberg, R. *Anal. Chem.* **2004**, *76*, 3638−3645.
(25) Chan, C. P.-y.; Haeussler, M.; Zhong, T. B.; Dong, Y.; Sin, K.-k.; Mak, W.-c.; Trau, D.; Seydack, M.; Renneberg, R. *J. Immunol. Methods* **2004**, *295*, 111−118.
(26) Mattoussi, H.; Mauro, J. M.; Goldman, E. R.; Anderson, G. P.; Sundar, V. C.; Mikulec, F. V.; Bawendi, M. G. *J. Am. Chem. Soc.* **2000**, *122*, 12142−12150.
(27) Goldman, E. R.; Anderson, G. P.; Tran, P. T.; Mattoussi, H.; Charles, P. T.; Mauro, J. M. *Anal. Chem.* **2002**, *74*, 841−847.
(28) Goldman, E. R.; Balighian, E. D.; Mattoussi, H.; Kuno, M. K.; Mauro, J. M.; Tran, P. T.; Anderson, G. P. *J. Am. Chem. Soc.* **2002**, *124*, 6378−6382.
(29) Gao, X. H.; Chan, W. C. W.; Nie, S. M. *J. Biomed. Opt.* **2002**, *7*, 532−537.
(30) Dosev, D.; Nichkova, M.; Liu, M.; Liu, G.-y.; Hammock, B. D.; Kennedy, I. M. *Proc. SPIE−Int. Soc. Opt. Eng.* **2005**, *5699*, 473−481.
(31) Nichkova, M.; Dosev, D.; Gee, S. J.; Hammock, B. D.; Kennedy, I. M. *Abstracts of Papers, 229th* ACS National Meeting, San Diego, CA, March 13−17, 2005; 2005; ANYL-095.
(32) Lvov, Y.; Ariga, K.; Onda, M.; Ichinose, I.; Kunitake, T. *Langmuir* **1997**, *13*, 6195−6203.
(33) Lvov, Y.; Munge, B.; Giraldo, O.; Ichinose, I.; Suib, S. L.; Rusling, J. F. *Langmuir* **2000**, *16*, 8850−8857.
(34) Cassagneau, T.; Fendler, J. H. *J. Phys. Chem. B* **1999**, *103*, 1789−1793.
(35) Trau, D.; Yang, W. J.; Seydack, M.; Caruso, F.; Yu, N. T.; Renneberg, R. *Anal. Chem.* **2002**, *74*, 5480−5486.
(36) Jacobson, B. S.; Cronin, J.; Branton, D. *Biochim. Biophys. Acta* **1978**, *506*, 81−96.
(37) Huang, N. P.; Michel, R.; Voros, J.; Textor, M.; Hofer, R.; Rossi, A.; Elbert, D. L.; Hubbell, J. A.; Spencer, N. D. *Langmuir* **2001**, *17*, 489−498.

Over the past several years, a soft lithographic technique called microcontact printing (μCP), originally developed by Whitesides et al. to transfer alkanethiolates onto gold substrates,[38,39] has been successfully applied to the direct patterning of proteins on a micrometer scale without loss of their biological activity on a variety of surfaces.[1,40−42] The μCP technique is relatively simple to perform in ordinary chemistry and biology research laboratories and does not require any special equipment or apparatus. Recently, micrometer-sized 2D protein arrays have been immobilized by microstamps and microwells for disease diagnosis and drug screening.[43]

The aim of this work is to develop new fluorophore biolabels with poly(L-lysine) encapsulation of Eu:Gd_2O_3 nanoparticles and to apply them to immunoassay microarrays prepared by the microcontact printing technique. The immunoassay for 3-phenoxybenzoic acid (PBA) is used as a model detection system to demonstrate the potential of this configuration for miniaturized assays and drug screening. PBA is a generic biomarker of human exposure to pyrethroids, a group of highly potent insecticides widely used in agriculture, forestry, horticulture, animal and public health, and households.[44] Confocal fluorescence imaging combined with internal standard calibration is used for obtaining quantitative data.

EXPERIMENTAL SECTION

Chemicals and Materials. Anti-rabbit IgG (whole molecule, developed in goat), rabbit IgG, sheep IgG, bovine serum albumin (BSA) and poly(L-lysine) hydrobromide (PL, average molecular weight of 66 700) were obtained from Sigma-Aldrich (St. Louis, MO). Fluorescein isothiocyanate (FITC) and PBA were purchased from Aldrich Chemical Co. (Milwaukee, WI) The preparation of the coating antigen PBA−BSA and the anti-PBA specific polyclonal antibody (As 294) has been reported previously.[44] The IgG fraction from the rabbit sera As294 was obtained by protein A purification using Affi-gel protein A MAPS II kit (Bio-Rad Laboratories). Rabbit IgG−fluorescein and BSA−fluorescein were prepared by a conjugation reaction between the amine groups of the protein and FITC following a standard procedure recommended by Molecular Probes (Eugene, OR).[45] The degree of labeling obtained for rabbit IgG−fluorescein was 6 mol of fluorescein/mol of IgG, and for BSA−fluorescein it was 3 mol of fluorescein/mol of IgG. Deionized water (18 MΩ·cm) was obtained using a Millipore purification system. Phosphate buffer saline (PBS) (pH 7.5) was 10 mM phosphate buffer, 0.8% saline. PBST was PBS with 0.05% Tween 20. Other buffers used were carbonate−bicarbonate buffer (pH 8.6), phosphate buffer (PB) (pH 7), borate buffer (pH 8), PB/citric acid (pH 6 and 7), and MES (pH 6). Black 96-well plates from Nunc (Roskilde, Denmark) were used for fluorescence measurements. Clay Adams cover glass from Fischer Scientific (Pittsburgh, PA) was used as the substrate for microcontact printing of proteins. The poly(dimethylsiloxane) (PDMS) stamp was prepared according to the literature method[46] using Sylgard 184 silicon elastomer (Dow Corning, Midland, MI). The stamp used in microcontact printing had a patterned matrix (1 cm^2) of 10-μm strips.

Instrumentation. The size and morphology of the Eu:Gd_2O_3 nanoparticles were determined using a Philips CM-12 transmission electron microscope (TEM). Particle size distributions were measured on a Nanotrac particle size analyzer, model NPA150 from Microtrac Inc. (Montgomeryville, PA), by dynamic light scattering technology. An ultrasonic bath 75D (VWR, Brisbane, CA) was used for preparation of the nanoparticle suspensions and for the cleaning procedures of the PDMS stamp and the glass substrates. Nanoparticle sizing was performed with a Sorvall RC5B Plus centrifuge (Kendro Laboratory Products, Asheville, NC)) and Eppendorf centrifuge 5415D (Brinkmann, Westbury, NY)). A Spectramax M2 cuvette/microplate reader (Molecular Devices, Sunnyvale, CA) was used for colloidal stability studies and for fluorescence quantification of the amino groups and the number of active binding sites on the surface of the biofunctionalized nanoparticles. Fluorescent images were acquired with a Leica TCS-SP laser scanning confocal microscope equipped with UV, argon, krypton, and helium−neon lasers for excitation and photomultiplier tubes (PMTs) for detection. Leica Confocal Software LCS Lite 2.0 was used for evaluation of the fluorescence intensity.

Preparation of Biofunctionalized Eu:Gd_2O_3 Nanoparticles. *Encapsulation of Eu:Gd_2O_3 Nanoparticles with Poly(L-lysine) Hydrobromide.* Eu:Gd_2O_3 nanoparticles (1 mg) were suspended using an ultrasonic bath in 1 mL of 10 mM PB (pH 7). Different amounts of PL solution corresponding to the range of 5−100 mg of PL/mg of nanoparticle was added to the particle suspension, and the mixture was incubated in a rotating mill for 2 h at room temperature. The excess polymer was removed by three cycles of centrifugation (5 min, 15000*g*) and redispersion.

Quantification of the Amino Groups on the Surface of the PL-Encapsulated Nanoparticles. The number of reactive amino groups on the surface of the PL-encapsulated nanoparticles was evaluated by their covalent coupling to FITC. The PL−Eu:Gd_2O_3 nanoparticles (1 mg) were suspended in 1 mL of carbonate−bicarbonate buffer (pH 8.6) and 100 μL of 25 mg mL^{-1} FITC solution in anhydrous dimethyl formamide was added. The coupling reaction took place for 1 h at room temperature in a rotating mill. The excess dye was removed by three cycles of centrifugation and washing of the nanoparticles with buffer. The fluorescein−PL−Eu:Gd_2O_3 nanoparticles were suspended in carbonate−bicarbonate buffer, and the fluorescence intensity of the fluorescein coupled to the amino groups was measured on the microplate reader (excitation 490 nm and emission 520 nm). A standard curve of FITC in carbonate−bicarbonate buffer measured in the presence of the same amount of noncoated nanoparticles was used for the quantification of the fluorescein bound to the particles.

Conjugation of the PL-Encapsulated Eu:Gd_2O_3 Nanoparticles with Antibodies. The carbohydrate residues of the IgG molecule (anti-PBA IgG, anti-rabbit IgG, or sheep IgG) (1 mg L^{-1}) were oxidized with 25 mM sodium periodate final concentration in 1 mL of PBS

(38) Xia, Y. N.; Whitesides, G. M. *Angew. Chem., Int. Ed.* **1998**, *37*, 551−575.
(39) Kane, R. S.; Takayama, S.; Ostuni, E.; Ingber, D. E.; Whitesides, G. M. *Biomaterials* **1999**, *20*, 2363−2376.
(40) Bernard, A.; Delamarche, E.; Schmid, H.; Michel, B.; Bosshard, H. R.; Biebuyck, H. *Langmuir* **1998**, *14*, 2225−2229.
(41) Graber, D. J.; Zieziulewicz, T. J.; Lawrence, D. A.; Shain, W.; Turner, J. N. *Langmuir* **2003**, *19*, 5431−5434.
(42) Tan, J. L.; Tien, J.; Chen, C. S. *Langmuir* **2002**, *18*, 519−523.
(43) Lin, S. C.; Tseng, F. G.; Huang, H. M.; Huang, C. Y.; Chieng, C. C. *Fresenius J. Anal. Chem.* **2001**, *371*, 202−208.
(44) Shan, G. M.; Huang, H. Z.; Stoutamire, D. W.; Gee, S. J.; Leng, G.; Hammock, B. D. *Chem. Res. Toxicol.* **2004**, *17*, 218−225.
(45) Molecular Probes. *Amine-reactive Probes*; http://www.probes.com.
(46) Kumar, A.; Whitesides, G. M. *Appl. Phys. Lett.* **1993**, *63*, 2002−2004.

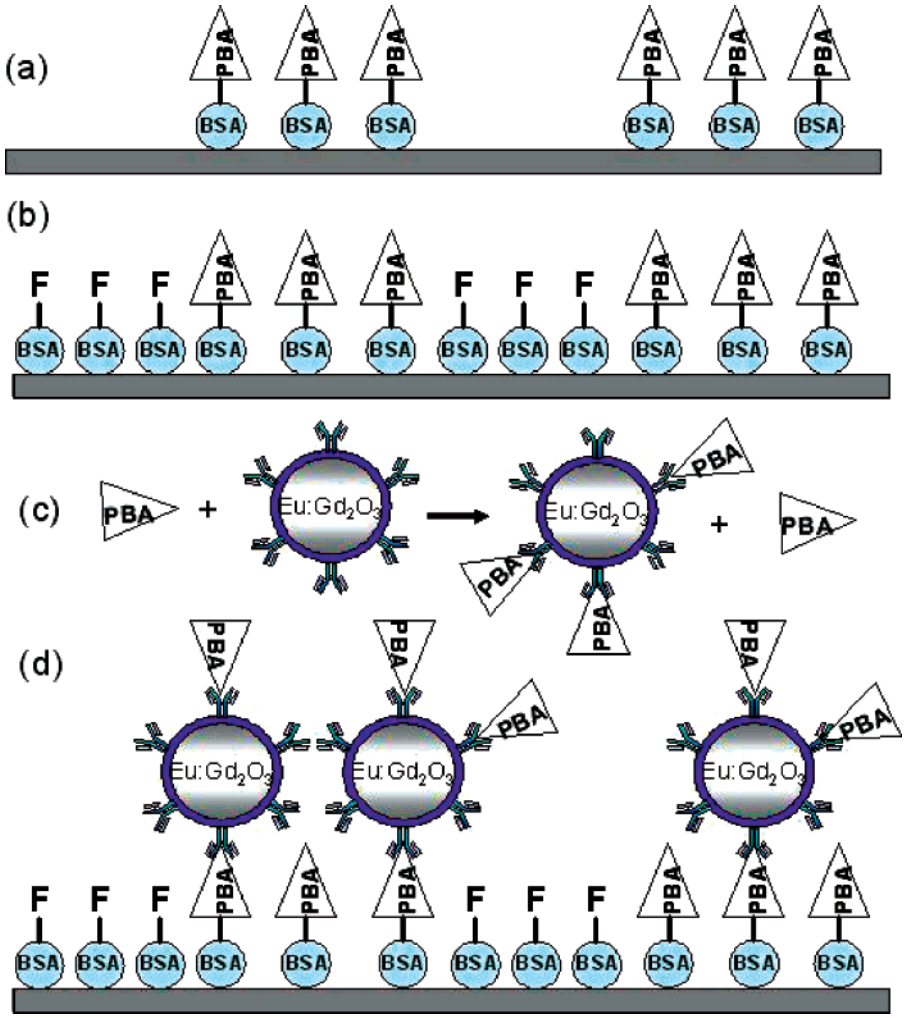

Figure 1. Principle of the microimmunoassay using Eu:Gd_2O_3 as biolabels and fluorescein as internal standard: (a) microcontact printing of the coating antigen (BSA−PBA), (b) immobilization of the internal standard (BSA−fluorescein), (c) preincubation of the labeled antibody with the analyte (PBA), and (d) incubation of the micropatterns with the labeled antibody.

for 30 min protected from light. After exchange to carbonate buffer (pH 8.6) by centrifugation with a Microcon centrifugal device (Millipore, Bedford, MA), the oxidized IgG (0.5 mg) was added to a suspension of 1.5 mg of PL−Eu:Gd_2O_3 nanoparticles in 1 mL of carbonate buffer to react with the amino groups for 2 h at room temperature in a rotating mill. Sodium cyanoborohydride (5 μL, 5 M) was added for the stabilization of the Schiff bases formed between the amine-coated nanoparticles and the aldehydes of the antibodies. After 30 min, the unreacted aldehyde sites were blocked for 30 min by addition of 10 μL of 1 M ethanolamine. The IgG−nanoparticle conjugate was purified from the reaction mixture by several buffer washings with PB (pH 7). To reduce the effect of nonspecific binding in the subsequent immunoassay, the antibody-conjugated nanoparticles were blocked with 0.5 mg L^{-1} BSA solution in 1 mL of 25 mM PB for 1 h at room temperature in the rotating mill. Following three consecutive washings, the resulting IgG−PL−Eu:Gd_2O_3 bioconjugates were used for the microimmunoassays.

Quantification of the Active Binding Sites on the Surface of the IgG−PL−Eu:Gd_2O_3 Nanoparticles. The number of active binding sites on the surface of the anti-rabbit IgG−PL−Eu:Gd_2O_3 nanoparticles was determined by using rabbit IgG labeled with fluorescein and measuring the fluorescence of the particle-bound rabbit IgG−fluorescein. The anti-rabbit IgG−PL−nanoparticle conjugate was incubated for 2 h in a rotating mill with 100 μg mL^{-1} IgG−fluorescein in PBST buffer. The particles were separated from the free IgG−fluorescein by three washings. Negative controls were prepared by exchanging the anti-rabbit IgG with sheep IgG in the conjugation reaction. Samples were run in duplicate. A standard curve of IgG−fluorescein in carbonate−bicarbonate buffer measured in the presence of the same amount of noncoated nanoparticles was used for quantification of the number of active binding sites on the nanoparticle surface.

Fluorescence Microimmunoassay for PBA with Internal Calibration. *Microcontact Printing of the Coating Antigen (BSA−PBA) onto the Glass Substrate.* Cover glass was used as a solid substrate for microcontact printing of the coating antigen BSA−PBA. Prior to use, the glass substrate was cleaned by immersion in a solution of H_2SO_4/H_2O_2 (70:30 v/v) for 2 h and then washed extensively in running deionized water. Then the substrate was thoroughly washed in an ultrasonic bath in ethanol and deionized water for 10 min each. Finally, it was dried under a blowing nitrogen stream. The PDMS stamp was washed by sonication in ethanol (3 × 10 min), dried under nitrogen, and exposed to the solution of the inking protein (50 μg mL^{-1} BSA−PBA in PBS) for 40 min. Excess solution was removed, and the stamp was dried

under nitrogen. After inking, the stamp was brought into contact with the glass substrate and a very small amount of force was applied to make a good contact between both surfaces.

Competitive Microimmunoassay. The BSA−PBA printing stage is schematically presented in Figure 1a. Printed slides were blocked with 2 mg mL^{-1} BSA (BSA−fluorescein) solution in PBS for 1 h and rinsed with water (Figure 1b). The substrates were then incubated in a shaker for 2 h with a suspension of the anti-PBA IgG−PL−Eu:Gd_2O_3 nanoparticles in carbonate−bicarbonate buffer (1 mg of particles/mL), allowing the specific interaction between antibody and antigen to occur (Figure 1c). In the case of PBA competition, the anti-PBA IgG−PL−Eu:Gd_2O_3 nanoparticles were preincubated for 5 h with PBA at different concentrations (from 0 to 500 $\mu g\ L^{-1}$) and then added to the glass substrate. After the interaction took place, the substrate was rinsed with buffer, water, dried under nitrogen, and scanned for fluorescence evaluation.

Scanning and Evaluation. A laser beam at 488 nm was used for the excitation of Eu:Gd_2O_3 nanoparticles and FITC. The detection wavelength ranges of the two PMTs were independently adjusted to 510−540 nm for FITC and 605−630 nm for the Eu:Gd_2O_3 nanoparticles. The gain of each PMT was individually adjusted to obtain equal signals from the FITC-dyed strips and the strips with maximal concentration of immobilized Eu:Gd_2O_3 nanoparticles (at zero PBA concentration). The experimentally determined gains of the two PMTs were used in the luminescence measurements in the competitive immunoassay. To reduce the experimental error, the average intensity of four strips was calculated for FITC and for Eu:Gd_2O_3 strips. Two substrates were analyzed for each experimental condition and four different areas were studied on each sample.

RESULTS AND DISCUSSION

Properties of the Eu:Gd_2O_3 Nanoparticles. Fluorescent Eu^{3+}-doped Gd_2O_3 nanoparticles were synthesized by spray pyrolysis according to our published procedure.[30,47] The level of doping was optimized previously, and it corresponds to 20% europium doping. The fluorescence lifetime of the nanoparticles is ~1 ms, allowing time-resolved measurements. The time-resolved fluorescence spectra of the nanoparticles in aqueous solution are presented in Figure 2. The photoluminescence emission spectrum shows that the nanoparticles have a characteristic bright red emission peak centered at 615 nm, which corresponds to the $^5D_0 \rightarrow {}^7F_2$ transition of the Eu^{3+} ion in the Gd_2O_3 crystal lattice (see Figure 2B). The full width half-maximum (fwhm) of the peak is 5 nm, which is very narrow in comparison with other fluorophores. The excitation spectrum reveals multiple excitation peaks far from the emission at 615 nm (see Figure 2A). The most efficient excitation is in the UV range between 250 and 280 nm. Some additional excitation peaks are distributed in the range 350−400 and 450−550 nm, respectively. This offers the possibility to choose between different excitation sources according to the experimental setup and the application. These spectral properties are nearly identical to those of the commercially available polystyrene nanoparticles doped with Eu chelates. Nevertheless, we found that the Eu:Gd_2O_3 nanoparticles have superior photostability under laser exposure.[48] This makes them more attractive for applications

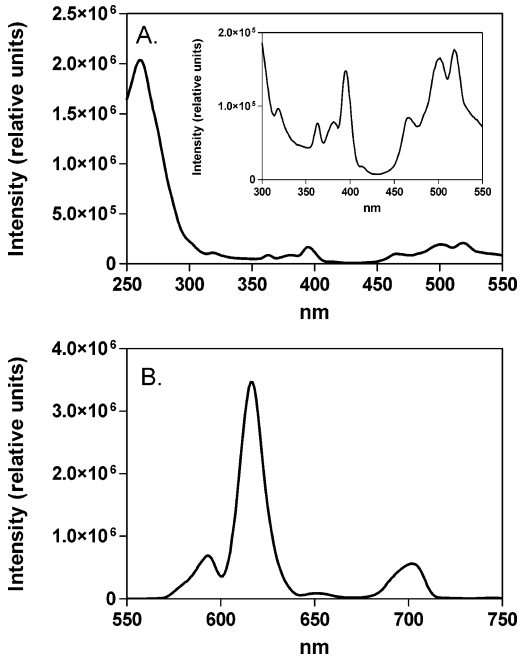

Figure 2. Fluorescence spectra: (A) excitation spectra at 615 nm and (B) emission spectra at 260 nm of Eu:Gd_2O_3 nanoparticles in PBS solution acquired in a plate reader.

using laser-induced fluorescence (e.g., confocal fluorescence microscopy).

Most of the as-synthesized particles have sizes between 5 and 500 nm and have nearly spherical shapes according to TEM analysis. A narrower size range was obtained by selective centrifugation. The sized nanoparticles used in this work were in the range of 5−200 nm. The TEM bright-field image of the sized nanoparticles is shown in Figure 3A, where several individual particles with sizes between 10 and 100 nm are observed. In addition, the size distribution of an aqueous suspension of the nanoparticles was determined by dynamic light-scattering measurements. Figure 4 presents the particle size distribution and the cumulative mass distribution. Most of the Eu:Gd_2O_3 is contained in particles with a diameter of 120 nm. Approximately 90% of the material was found to be in particles smaller than 187 nm, and we conclude that a corresponding 90% of the luminescent signal derived from particles less than 187 nm. As expected, particles smaller than 40 nm were not detected by this technique due to limitations of the instrument. It should be noted that the optical emission from these nanoparticles does not vary with particle size as quantum dots do. Hence, the lack of monodispersity is not an impediment to their application in our assays.

Encapsulation of the Eu:Gd_2O_3 Nanoparticles with PL and Conjugation to Antibodies. As mentioned in the introduction, the polycationic polymer PL has been shown to chemisorb on anionic surfaces, including various metal oxide surfaces.[37] Similarly, we were able to coat the Eu:Gd_2O_3 nanoparticles with a layer of PL based on the electrostatic attraction between the surface OH groups and the charged amino acid residues by incubation of the nanoparticle suspension in PL aqueous solution. The resulting PL-encapsulated nanoparticles can be easily sepa-

(47) Dosev, D.; Guo, B.; Kennedy, I. M. *J. Aerosol Sci*, in press.

(48) Dosev, D.; Nichkova, M.; Liu, M.; Liu, G.-y.; Hammock, B. D.; Kennedy, I. M. *J. Biomed. Opt.*, in press.

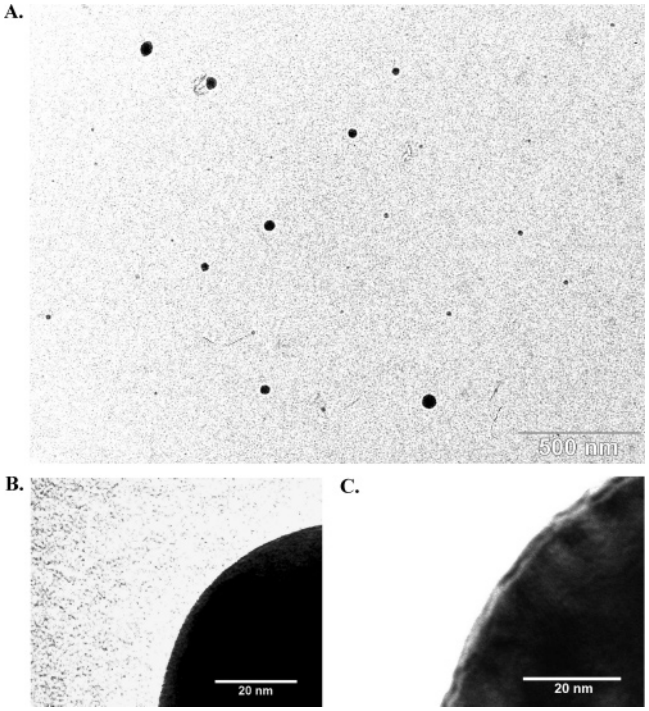

Figure 3. TEM images of Eu:Gd_2O_3 nanoparticles: (A) overview of noncoated sized nanoparticles; (B) high-resolution image of the bare surface of noncoated nanoparticle; (C) high-resolution image of the poly(L-lysine) shell on the surface of the poly(L-lysine)-encapsulated nanoparticle.

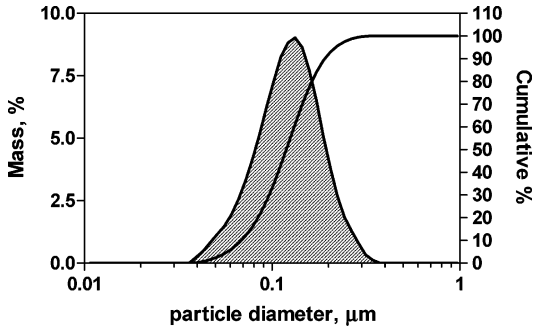

Figure 4. Particle size and mass distributions of aqueous suspension of the Eu:Gd_2O_3 nanoparticles determined by light-scattering measurements.

rated from the excess polymer in the PL coating solution by centrifugation. The formation of a PL layer was confirmed by TEM analysis, colloidal stability studies, and determination of the free amino groups on the surface of the encapsulated nanoparticles. The high magnification TEM images of the surface of bare and PL-encapsulated nanoparticles are presented in Figure 3B and C, respectively. It can be clearly observed that a PL layer was assembled onto the nanoparticles' surface. The measured thickness of the polymer shell is about 1−2 nm, and it is negligible when compared to the total size of the nanoparticles. The observed thickness of the PL shell is similar to the previously reported thickness of an electrostatically adsorbed PL monolayer formed on a mercaptoundecanoic acid-modified gold surface measured with surface plasmon resonance.[49] The PL encapsulation did not

(49) Jordan, C. E.; Frey, B. L.; Kornguth, S.; Corn, R. M. *Langmuir* **1994**, *10*, 3642−3648.

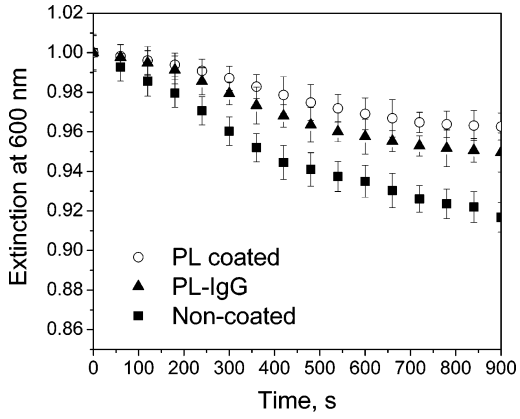

Figure 5. Colloidal stability of suspensions of naked, PL-encapsulated, and PL−IgG−functionalized Eu:Gd_2O_3 nanoparticles in 25 mM phosphate buffer, pH 7. Nanoparticles (0.5 mg) were suspended in 1 mL of buffer, and the extinction at 600 nm was monitored with the time. Standard deviations correspond to four measurements.

cause any noticeable change in the morphology and size distribution of the nanoparticles.

For Y_2O_3 particles of size and density similar to those of the Gd_2O_3 nanoparticles, it has been reported that the turbidity of a suspension of the material should increase on aggregation.[50] Thus, we used optical absorbance data to study the colloidal stability of bare and PL-encapsulated nanoparticle suspensions. The aggregation kinetics of both suspensions in PB (pH 7.5) was evaluated by measuring their light extinction at 600 nm as a function of time (see Figure 5). It can be seen that faster aggregation takes place for the suspension of bare particles. The adsorbed PL layer caused the nanoparticles to disperse in the buffer and prevented their aggregation, hence conferring higher colloidal stability due to electrostatic and steric interactions.[51] Aggregates of nanoparticles in colloidal solutions were formed due to van der Waals attractive forces, which are opposite to the repelling electrostatic forces. Surface coating of the nanoparticles should lead to changes in their surface charge and therefore in their colloidal stability. The difference in the colloidal stability of bare and PL-coated nanoparticles can be considered as an independent proof of the formation of the PL layer.

The main function of the PL coating is to provide a suitable interface for the attachment of the nanoparticles to biomolecules. The reactive amino (lysine) groups on the surface of the PL-encapsulated nanoparticles were detected by their covalent coupling to FITC (see Figure 6a, b). The amount of fluorescein bound to the particle surface was determined with a FITC standard curve considering a binding ratio of fluorescein/amino groups of 1:1. The FITC standard curve was measured in the presence of noncoated nanoparticles and was linear (R^2 of 0.999), indicating that the standards used were below the self-quenching concentration of the dye. The presence of the same amount of nanoparticles in the standards as in the samples assured that the standard curve was corrected for the light extinction caused by the particles. The FITC test is straightforward and easy to perform. The high specific weight of the Eu:Gd_2O_3 nanoparticles (~7.4 g/cm^3) allows very

(50) Plaza, R. C.; Quirantes, A.; Delgado, A. V. *J. Colloid Interface Sci.* **2002**, *252*, 102−108.

(51) Bruemmel, Y.; Chan, C. P. Y.; Renneberg, R.; Thuenemann, A.; Seydack, M. *Langmuir* **2004**, *20*, 9371−9379.

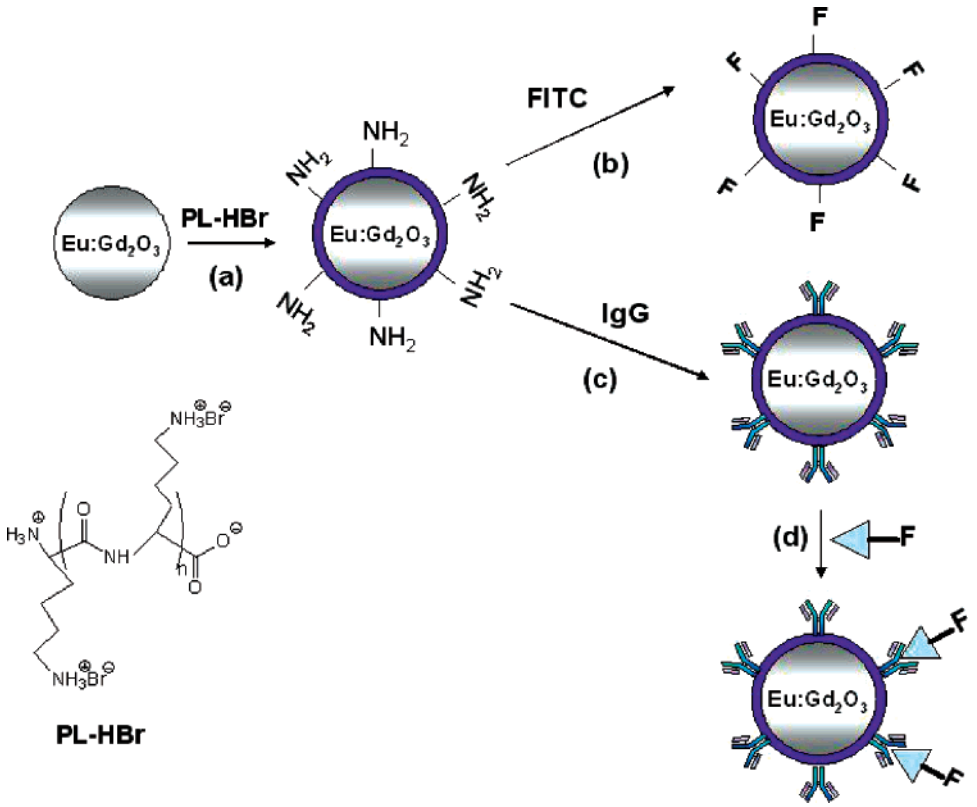

Figure 6. Schematic illustration of the preparation of biofunctional Eu:Gd_2O_3 nanoparticles: (a) encapsulation with poly(L-lysine) hydrobromide (PL), (b) quantification of amino groups by coupling to fluorescein isothiocyanate (FITC); fluorescein (F), (c) covalent coupling to oxidized antibody (IgG), and (d) quantification of antibody binding sites by fluorescein-labeled antigen.

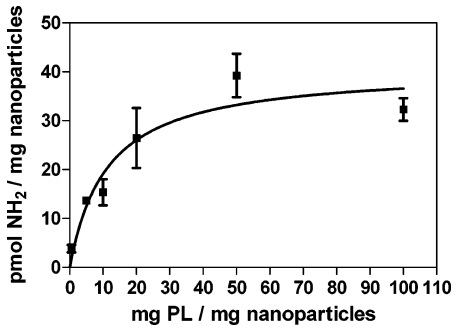

Figure 7. Number of amino groups on the surface of the PL-encapsulated Eu:Gd_2O_3 nanoparticles as a function of the amount of poly(L-lysine) polymer used for their coating as determined by the FITC test.

easy separation procedures by centrifugation. The efficient removal of the excess FITC was proven by measuring the fluorescence of the washing buffer. This guaranteed that the measured fluorescence signal was only due to the fluorescein bound to the PL layer. We have experimentally determined the amount of PL needed for complete encapsulation of 1 mg of nanoparticles. The number of available reactive amino groups was determined by the FITC test for 2-h coating procedures using different amounts of PL (see Figure 7). The saturation of the surface corresponds to a coating concentration of ~30 mg of PL/mg of nanoparticles and it results in ~30−35 pmol of NH_2 groups/mg of nanoparticles. Similar surface densities can be achieved using smaller amounts of PL but for longer (overnight) coating times (data not shown).

The stability of the polymer coating of the nanoparticles is another important issue in their application as fluorophore labels in biosassays. We tested the stability of the PL layer in some of the most commonly used buffers and also in the reaction conditions used for covalent coupling to oxidized antibodies. The number of amino groups was quantified before and after these treatments. The PL encapsulation was stable for several days in PBS (pH 7.5), borate buffer (pH 8), PB/citric (pH 6 and 7), and MES (pH 6). No loss of lysines was observed during "blank" conjugation reactions performed without adding the antibody. Therefore, the PL encapsulation method developed here provides suitable surface functionality for further biomolecule conjugation.

With a view to use the Eu:Gd_2O_3 nanoparticles as reporters in microimmunoassays, we immobilized antibodies (anti-rabbit, sheep, anti-PBA IgGs) onto the PL-encapsulated particles via covalent binding between the available amino groups of the polymer and the aldehyde-activated antibodies (see Figure 6c). The main advantage of this method is the site-specific oriented immobilization of the IgG molecules through their Fc region without affecting their activity. Fluorescent measurements showed that the excitation and emission spectra of bare and antibody-conjugated nanoparticles were identical (data not shown). Furthermore, the colloidal stability of the antibody−nanoparticle conjugates was slightly lower than that of the PL-encapsulated nanoparticles (see Figure 5).

Anti-rabbit IgG was used to optimize the coupling reaction between the antibodies oxidized by periodate and the PL-encapsulated nanoparticles containing 30−35 pmol of amino groups/mg of particles. The immunoreactivity of the immobilized

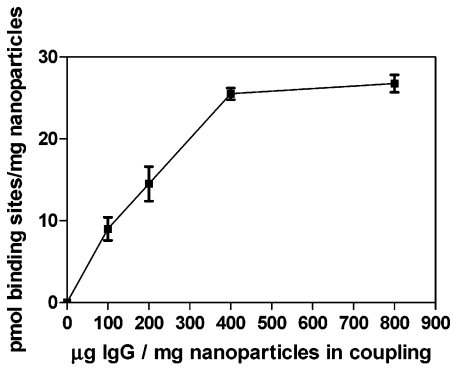

Figure 8. Active antibody binding sites on the surface of the Eu:Gd_2O_3 nanoparticles as a function of the amount of antibody used in the conjugation reaction. Anti-rabbit IgG was covalently coupled to the PL-encapsulated nanoparticles, and the binding sites were detected by interaction with rabbit IgG−fluorescein.

anti-rabbit IgGs was tested by their interaction with rabbit IgG labeled with fluorescein. The number of active binding sites on the surface of the anti-rabbit IgG−PL−Eu:Gd_2O_3 nanoparticles was determined by measuring the fluorescence of the rabbit IgG−fluorescein bound to the particles. Sheep IgG−PL−Eu:Gd_2O_3 particles were used as negative control. The number of anti-rabbit IgG binding sites as a function of the amount of antibody used in the conjugation reaction is presented in Figure 8. A saturation of ~28 pmol of binding sites can be observed when using 400 μg of IgG/mg of particles in the coupling reaction. The maximum amount of antibodies that can be immobilized is close to the total amount of reactive amine groups of the PL layer (~30−35 pmol of NH_2 groups/mg of nanoparticles) determined by the FITC test described above. Coupling conditions corresponding to 20 pmol of IgG/mg of nanoparticles (70% of the particle surface saturation) were selected for the conjugation of anti-PBA rabbit IgG to PL−Eu:Gd_2O_3 and their application to the fluorescence microimmunoassay. It was anticipated that 70% surface coverage of the nanoparticles with active antibodies would enable the complete binding of the particles to the micropatterns, providing enough luminescence signal and good sensitivity of the immunoassay.

We would like to note that the PL encapsulation of the nanoparticles presented here is a versatile method that allows the preparation of conjugates with different proteins and small molecules. In addition to the antibody labeling, we have also obtained biotinylated nanoparticles by conjugation of the lysine groups to biotin−NHS. The presence of biotin molecules on the particle surface was detected with streptavidin−Alexa Fluor 647 (data not shown). In another experiment, avidin was covalently attached to the amino groups of the PL-encapsulated nanoparticles via glutaraldehyde cross-linking and the conjugate was successfully applied to the visualization of BSA−biotin printed micropatterns (data not shown). The biotinylated and avidinated nanoparticles can be used as fluorescent reporters in a variety of bioassays.

Fluorescence Microimmunoassay for PBA with Internal Calibration. To demonstrate the potential of the fluorescent biofunctionalized nanoparticles as labels in miniaturized immunoassays, we used as a model system the immunodetection of PBA, a common metabolite of many pyrethroid insecticides. The fluorescence microimmunoassay for PBA developed here was based on an indirect competitive format where the coating antigen (BSA−PBA) was micropatterned on a glass substrate, the anti-PBA antibody was labeled with PL-encapsulated Eu:Gd_2O_3 nanoparticles as described above, and BSA−fluorescein was used for internal fluorescence calibration. The preparation of the BSA−PBA micropatterns and the immunoreaction is schematically presented in Figure 1. The printing conditions for BSA−PBA (concentration, buffer, contact time, etc.) were chosen according to the reported procedures for protein μCP.[40,41] PBS was used as a printing buffer because its pH is suitable for maintaining the biological activity of the printed proteins. To test the protein-transfer efficiency of BSA−PBA in the μCP, we initially printed BSA labeled with fluorescein. The fluorescence images corresponded to the dimensions and the pattern of the elastomeric stamp (10 μm × 10 μm) and exhibited uniform fluorescence intensity.

To test the antigen-binding capabilities of the anti-PBA IgG−PL−Eu:Gd_2O_3 nanoparticle conjugates, a glass substrate patterned with BSA−PBA and blocked with BSA was incubated for 1 h with the nanoparticle suspension (1 mg of particles/mL; 20 pmol of IgG/mg of nanoparticles). The fluorescent image and the corresponding line intensity profile of the obtained micropatterns are shown in Figure 9A. A series of alternating bright (red) and dark strips can be observed. The actual width of the strips (10 μm) is defined by the PDMS stamp used. The red strips correspond to the fluorescent nanoparticles specifically bound to the printed BSA−PBA, and the dark strips correspond to the BSA-blocked spacings between them. The average signal-to-noise ratio, i.e., specific intensity/background intensity of 6−8 demonstrates successful immunoreaction with very low nonspecific binding. Therefore, nonspecific deposition of the nanoparticles was successfully prevented by blocking both the bare glass substrate and the nanoparticles with BSA.

One of the limitations of the quantitative measurements performed by fluorescence microscopy is the lack of internal calibration. Quantitative measurement is limited to the comparison of signals within the same sample, where variation of sample preparation is excluded.[7] Therefore, for quantitative competitive microimmunoassays, we introduced an internal calibration with bath-adsorbed BSA−fluorescein. It has been reported that μCP of proteins and adsorption of proteins from solution are equivalent and similar densities can be achieved.[40,41,52] Thus, to perform the quantitative immunoassay in a microarray format, after printing the antigen (BSA−PBA), the bare glass surface was coated by physical adsorption from a solution of BSA−fluorescein. BSA−fluorescein had two functions: as a blocking agent to reduce nonspecific binding and as an internal fluorescent standard (see Figure 1b). Using 2 mg mL^{-1} protein solution in PBS we obtained reproducible fluorescence signals from bath-adsorbed BSA−fluorescein.

The competitive immunoassay for PBA was carried out with a 5-h preincubation of the labeled antibody (anti-PBA IgG−PL−Eu:Gd_2O_3) with different PBA concentrations ranging from 0 to 500 μg L^{-1} (see Figure 1c). The glass substrates (printed BSA−PBA/blocked BSA−fluorescein) were incubated with these solutions for 1 h where the nonsaturated binding sites of the labeled antibody bind to the printed PBA. Representative fluorescence

(52) Feng, J.; Gao, C. Y.; Wang, B.; Shen, J. C. *Thin Solid Films* **2004**, *460*, 286−290.

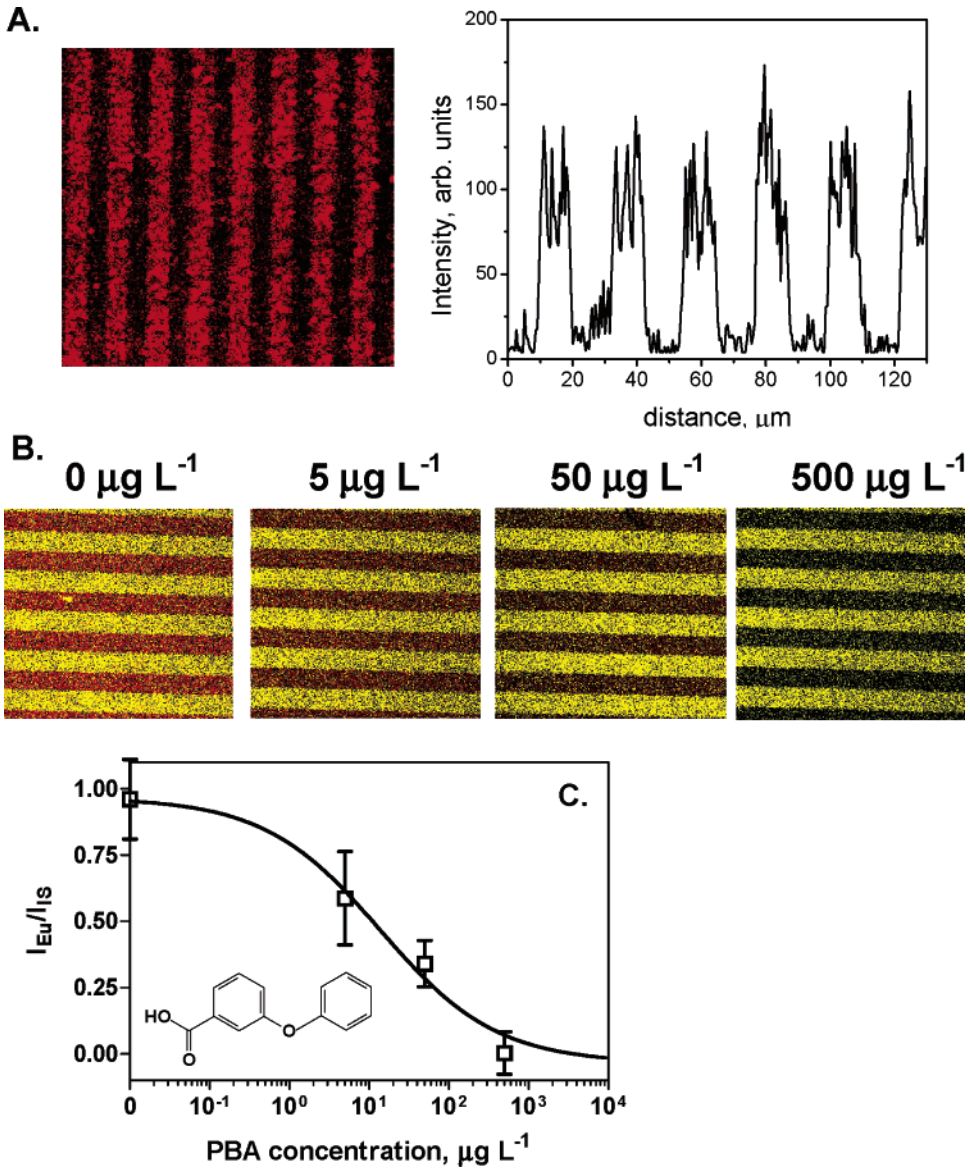

Figure 9. Microimmunoassay for PBA. (A) Fluorescence image of anti-PBA IgG−PL−Eu:Gd_2O_3 nanoparticles bound to microcontact-printed BSA−PBA onto a glass substrate. The nonprinted surface was blocked with BSA. The fluorescence intensity profile corresponds to an average signal of 102 ± 35 arbitrary units (5 strips). (B) Fluorescence images of glass substrates printed with BSA−PBA, blocked with BSA−fluorescein as internal standard and incubated with anti-PBA IgG−PL−Eu:Gd_2O_3 nanoparticles and four concentrations of PBA ranging from 0 to 500 μg L^{-1}. (C) Standard curve for the PBA microimmunoassay. Two substrates were analyzed for each PBA concentration and four different areas were studied on each sample. The average intensity of four strips was calculated for FITC and for Eu:Gd_2O_3 strips; inset: structure of 3-phenoxybenzoic acid (PBA).

images of the patterns obtained for the PBA concentrations tested are shown in Figure 9B. The yellow strips correspond to the internal standard (fluorescein) fluorescence, which has similar intensity for the four substrates. Increasing PBA concentration leads to smaller amounts of nanoparticles bound on the printed BSA−PBA strips and therefore to a decrease in the red Eu:Gd_2O_3 fluorescence intensity. The resulting dependence of the normalized specific fluorescence signal (I_{Eu}/I_{IS}) versus the PBA concentration is presented in Figure 9C. The parameters of the sigmoidal fit of the competitive immunoassay are as follows: IC50 = 14 μg L^{-1}, slope −0.6, and R^2 = 0.987. The detection limit defined as 20% inhibition corresponds to 1.4 μg L^{-1} PBA, which is comparable with the reported ELISA for the same analyte.[44] The presented detection system is a proof of concept for an microimmunoassay using lanthanide oxide as fluorescent reporter. The assay could be further optimized in regard to several parameters such as the amount of nanoparticles used, antibody surface density of the coated nanoparticles, amount of printed BSA−PBA, incubation time, etc. A narrower size distribution and better colloidal stability of the nanoparticles could lead to improvement in sensitivity and reproducibility. The microarray immunoassay configuration has the potential to be part of a miniaturized high-throughput portable device using multichannel PMT or CCD camera for detection. Furthermore, the microimmunoassay presented here can be easily extended to multianalyte assays with labels with narrow emission spectra, such as lanthanides or quantum dots.

CONCLUSIONS

Crystalline nanoparticles of Eu^{3+}-doped gadolinium oxide were used for the first time as luminescent labels in a competitive

microarray immunoassay for phenoxybenzoic acid. Their unique spectral properties, such as excellent photostability and long lifetime, and their low-cost production, make them an attractive alternative to conventional fluorophores used as reporters in immunoassays.

The surface properties of the metal oxide nanoparticles, such as Eu:Gd_2O_3, facilitate their easy amino functionalization by stable encapsulation with the polycationic polymer poly(L-lysine). The PL encapsulation does not affect the fluorescence of the nanoparticles and increases their colloidal stability in aqueous suspensions. Stable bioconjugates between the PL-coated particles and specific antibodies were obtained by controlling the number of active binding sites on the particle surface. The PL coating layer could be modified not only by reaction of the amine groups with various molecules but also by replacement of some of the lysine residues with other amino acids. In this way, modified PL may lead to a versatile route for the specific immobilization of protein and small molecules (e.g., biotin, haptens) onto the metal oxide surfaces of the nanoparticles. Furthermore, the effective encapsulation of the Eu:Gd_2O_3 nanoparticles with PL could be extended to the use of polycationic poly(ethylene glycol) grafted copolymers, such as PL-*g*-PEG, to induce resistance to nonspecific protein adsorption in binding assays performed in biological samples.[37,53] Finally, PL is known to bind tumor cells with high affinity both in vitro and in vivo, and thereby, PL-encapsulated nanoparticles might find another application as a primary component in the construction of targeting agents.[54]

Most of the reported immunodetection methods with fluorescent nanolabels have focused on sandwich immunoassays performed in 96-well plates. Here we present the successful application of the PL-encapsulated Eu:Gd_2O_3 nanoparticles to the detection of the pyrethroid metabolite PBA in a microarray format fabricated by a microcontact printing technique. The nonoptimized competitive microarray immunoassay has sensitivity comparable with the conventional ELISA for this target analyte. Blocking the surface of the nanoparticles and the glass substrate by BSA is a key step for the successful immunoreaction with low nonspecific binding. The use of microcontact printing allows the introduction of an internal standard calibration in the quantitative measurements and allows us to overcome one of the limitations of fluorescence detection—the lack of a reference signal. We anticipate that the new luminescent biolabels may find diverse biotechnology applications, especially in biosensors, protein microarrays, enzyme assays, and high-throughput screening assays.

ACKNOWLEDGMENT

The authors acknowledge the support of the National Science Foundation, Grant DBI-0102662, and the Superfund Basic Research Program with Grant 5P42ES04699 from the National Institute of Environmental Health Sciences, NIH.

Received for review May 12, 2005. Accepted August 24, 2005.

AC050826P

(53) Kenausis, G. L.; Voros, J.; Elbert, D. L.; Huang, N. P.; Hofer, R.; Ruiz-Taylor, L.; Textor, M.; Hubbell, J. A.; Spencer, N. D. *J. Phys. Chem. B* **2000**, *104*, 3298−3309.

(54) Ryser, H. J. P.; Mandel, R.; Hacobian, A.; Shen, W. C. *J. Cell. Physiol.* **1988**, *135*, 277−284.